# ULTRASONIC CHARACTERIZATION OF STRUCTURAL PROPERTIES OF ORIENTED STRANDBOARD: A COMPARISON OF DIRECT-CONTACT AND NON-CONTACT METHODS[1]

*Ronnie Y. Vun*†
Graduate Research Assistant

*Qinglin Wu*†
Associate Professor
Louisiana Forest Products Laboratory
School of Renewable Natural Resources
Louisiana State University Agricultural Center
Baton Rouge, LA 70803

*Mahesh C. Bhardwaj*
Research and Development Director

and

*Gary Stead*
President
SecondWave Systems Corporation
1020 East Boal Avenue
Boalsburg, PA 16827

(Received January 2002)

ABSTRACT

A through-thickness ultrasonic transmission (UT) in oriented strandboard (OSB) was done to compare the performance of direct-contact (DC) and non-contact (NC) ultrasonic systems. The DC measurements produced a higher velocity than the NC system for a given board type, possibly due to transducer's compression over liquid couplant in the DC method. The UT responses correlated nonlinearly to sample density. The responses were not affected by the panel shelling ratio for the three-layer boards. Viable correlations between panel properties and UT parameters were board-specific for either method. Attenuation and root means square voltage (RMS) parameters were suitably used as density predictors if the flake alignment level is known; otherwise, velocity parameter could be used. In the single-layer boards, internal bond strength, bending stiffness, and breaking resistance were highly correlated to attenuation and RMS, a calibration importance. A density of 900 kg/m$^3$ marked the transition point for the UT responses. The point showed the transition between the diminishing physical effects of the interspatial voids in the lower density half and the increasing plastic-strain hardening modifications in the higher density half. The high correlations of DC-Velocity and NC-Attenuation to density and strength properties attest a feasible application of both methods in wood composite research and in a real-time quality control system for fiber-based facilities.

*Keywords:* Densification, direct-contact, non-contact ultrasound, quality control, OSB, velocity, attenuation.

## INTRODUCTION

Oriented strandboard (OSB) is one of the modern structural wood composites widely used as sheathing, flooring, and I-joist materials in house construction. OSB consists of wood strands or flakes glued with an exterior-type, waterproof resin. Mat layering and alignment of wood flakes are used to improve mechanical properties of the board. The mat formation by depositing resin-coated flakes re-

[1] This paper (NO: 02-40-0457) is published with the approval of the Director of the Louisiana Agricultural Experiment Station.

† Member of SWST.

*Wood and Fiber Science*, 35(3), 2003, pp. 381–396

panels were fabricated for the study (Wu 1999; Lee and Wu 2002). Panels in each type were made with 0.5% wax at the 4% RC level (based on oven-dry weight of the wood flakes) in two replicates. The single-layer boards had four nominal densities (450, 650, 850, and 1150 kg/m$^3$), and three alignment levels. The three-layer boards had four shelling ratios (represented by flake weight ratio, FWR, between the face layers and the entire panel), and two alignment levels. The single-layer panels (610 × 610 × 13 mm) were prepressed to thickness prior to heating of the mats for resin curing at 190°C for 6 min. The three-layer panels (610 × 610 × 13 mm) were made with a conventional pressing procedure (one-min closing and 6-min pressing time at 190°C). After hot pressing, the panels were conditioned and edge-trimmed. Based on the measured flake angles from panel surface, flake alignment levels were quantified using percent of alignment (Geimer 1979). The flake alignment level was classified into three categories: (1) high alignment level (HAL), which ranged from 76 to 85%, (2) low alignment level (LAL), from 56 to 59%, and (3) random alignment level (RAL), from 22 to 29%. Ten base specimens (51 × 51 × 13 mm) were randomly selected and cut from each panel replicate, giving a total of twenty samples at each condition. The major flake alignment direction of the panel was marked on the top surface of each sample. The specimens were conditioned at 24°C and 60% relative humidity prior to the UT testing to reach an average equilibrium moisture content of 7.2% for all panels. Thereafter, the specimens were destructively evaluated for the mechanical properties.

### *Direct-contact transmission*

Direct-contact UT measurements were taken in a through-transmission mode with two Panametrics 100-kHz transducers—coupled on each opposite surface of the specimen using silicon gel (Fig. 1a) and a constant pressure under 3-kg weight. A Panametrics 5058 Pulser/Receiver was used to generate a 400-volt impulse that excites one transmitting transducer, and the other transducer captures the transmitted signal. Equipment calibration settings, including gain, damping, pulse height, pulser gain, and attenuator, were selected to cover the whole density range of the specimens tested. With a consistent setting of 40–60 dB gain or 0–80 dB attenuator, 30-dB preamplified signals were sampled at a rate of 5 MHz, and the signals were digitized by a GageScope 8-bit CS225 card and processed by a signal processing software.

Velocity, impedance, attenuation, and root mean square (RMS) voltage of the DC ultrasound parameters were used to characterize the properties of the OSB (Vun 1998). The through-thickness velocity, $V$(m/s), is the ratio between sample thickness and signal transit time:

$$V = d/t \tag{1}$$

where $d$ is the sample thickness (mm) and $t$ is the signal transit time (μs) across the thickness. The impedance of the material determines the alternating current of stress waves that flows through the material. As an analog to a given alternating current potential difference, the impedance of the ultrasonic current is affected by difference in sample density (Benson 1991). The material impedance, Z (Gg/s.m$^2$), is then calculated by

$$Z = V \cdot \rho \tag{2}$$

where ρ is the sample density ($10^{-3}$ kg/m$^3$). Attenuation is the energy loss associated with a decrease in the wave amplitude scattered by discontinuity and absorption among the different densities. Attenuation, α(dB), is given by

$$\alpha = 20 \text{ Log}(A/A_{ref}) \tag{3}$$

where $A$ is the peak amplitude (v), and $A_{ref}$ is the maximum amplitude allowable by the system (i.e., 5.2 volts). The RMS voltage represents the signal intensity of the acquired signal (Beauchamp and Yuen 1979), which is measured on a linear scale in voltage and computed by time-averaging rectification as

material (s), and $t_{12}$ is the ToF through air column when material is in between transducer 1 and transducer 2 (Fig. 1b).

The attenuation energy is determined by the integrated response (IR). IR (dB) is the net power of the actual ultrasound energy transmitted through the material as evaluated by:

$$IR_m = IR_a - IR_{12} \tag{7}$$

where $IR_m$ is the integrated response of the peak energy transmitted in the material, $IR_a$ is the IR in air, and $IR_{12}$ is the IR in air when the material is in between the transducers. Being frequency independent, IR is related to the transmission coefficient ($T$) that measures how ultrasound is transmitted from one medium to another, given by:

$$T = \frac{Z_1 Z_2}{(Z_1 + Z_2)^2} \tag{8}$$

where $Z_1$ and $Z_2$ are the acoustic impedance of ultrasonic propagation in medium 1 and medium 2, respectively. $IR_m$ is related to $T$ as

$$IR_m = 20\ \mathrm{Log}(T) \tag{9}$$

The variable $IR_m$ provides information on internal material quality such as degree of bonding, nature of the microstructure and texture, absence or presence of phases, and type of inclusions in the material (Bhardwaj 1997; Bhardwaj et al. 2000).

The UT measurement with the NCA1000 analyzer was done as follows. After the transducers were aligned, the equipment was calibrated to a known air ultrasound velocity of 344–346 m/s and a reference specimen, a 25.4-mm transparent polystyrene having 21.75 μs round trip ToF and 2320 m/s material velocity under ambient conditions. From the first peak analysis, gates were created forming four ultrasonic paths of propagation. These paths were P1: transducer 1 to transducer 2, P2: transducer 1 to material bottom surface reflection, P3: transducer 2 to material top surface reflection, and P4: transducer 2 to transducer 1. Then, based on the reference velocity and thickness, the velocity, thickness, and ToF of the test materials were computed and displayed.

### *Panel density and density profile*

Vertical (thickness) and horizontal (length or width) density profiles of each specimen were mapped using a Quintek Density Profiler (QDP-01X) after UT measurements. The maximum, average, and minimum densities along each direction were evaluated from the measured profiles for each sample.

### *Mechanical properties*

After UT and density measurements, each base specimen was ripped to obtain two *in-situ* 51 × 13 × 13-mm bending samples with the largest dimension of each sample parallel to the major flake alignment direction, and a 51 × 25 × 13-mm sample for testing internal bond (IB) strength. All tests were conducted with a 4260 Instron machine according to the ASTM-D1037. The IB tests were done at a strain rate of 1 mm/min; whereas the modulus of elasticity (MOE) and modulus of rupture (MOR) of each sample were measured with a 6 mm/min loading rate. Each failed specimen was oven-dried to determine its moisture content at the testing time. IB (MPa), bending stiffness (E·I, MPa.cm$^4$), and breaking resistance (R·S, MPa.cm$^3$) were computed as:

$$\mathrm{IB} = \frac{\mathrm{P}}{\mathrm{bL}} \tag{10}$$

$$\mathrm{E{\cdot}I} = \mathrm{MOE}\frac{\mathrm{bh}^3}{12} \tag{11}$$

$$\mathrm{R{\cdot}S} = \mathrm{MOR}\frac{\mathrm{bh}^2}{6} \tag{12}$$

where P is the peak load from the IB test (N), E is the MOE (MPa), I is the moment of inertia given by I = bh$^3$/12 (cm$^4$), R is the MOR (MPa), S is the section modulus given by S = bh$^2$/6 (cm$^3$), and $b$, $h$, and $L$ are the width, height, and length (cm) of the specimen, respectively.

TABLE 1. *Mechanical and ultrasonic properties for the single-layer boards at the 4% RC level.*

| Board[c] type | Density (kg/m$^3$) | Mechanical properties[b] MOR (MPa) | MOE (MPa) | RS (MPa·cm$^3$) | EI (MPa·cm$^4$) | Ultrasonic properties[d] IB (MPa) | DCV (m/s) | DCA (−dB) | DCR (v) | DCZ (Mg/s·m$^2$) | NCV (m/s) | NCA (−dB) |
|---|---|---|---|---|---|---|---|---|---|---|---|---|
| HAL | 594 | 30.4 | 243 | 9.9 | 51 | 0.64 | 810 | 28.25 | 0.31 | 481 | 610 | 83.0 |
| | (5)[a] | (2.1) | (20) | (0.6) | (5) | (0.18) | (112) | (5.5) | (0.06) | (67) | (7) | (6.1) |
| | 783 | 46.0 | 485 | 14.2 | 94 | 1.12 | 920 | 7.11 | 0.88 | 709 | 770 | 66.7 |
| | (79) | (6.3) | (133) | (2.0) | (26) | (0.18) | (61) | (6.0) | (0.28) | (127) | (66) | (2.2) |
| | 1043 | 65.1 | 1056 | 21.2 | 213 | 1.43 | 1326 | 1.23 | 1.11 | 1222 | 905 | 71.3 |
| | (41) | (5.6) | (214) | (2.2) | (46) | (0.05) | (160) | (0.4) | (0.07) | (375) | (83) | (4.1) |
| | 1207 | 68.4 | 1296 | 23.0 | 275 | 1.47 | 1257 | 0.75 | 1.23 | 1426 | 1075 | 84.0 |
| | (42) | (1.6) | (160) | (0.5) | (28) | (0.25) | (126) | (0.5) | (0.10) | (228) | (207) | (6.0) |
| LAL | 562 | 21.0 | 185 | 7.0 | 40 | 0.57 | 748 | 32.13 | 0.24 | 421 | 1046 | 87.8 |
| | (22) | (1.5) | (12) | (0.7) | (3) | (0.12) | (32) | (7.5) | (0.11) | (22) | (364) | (5.0) |
| | 808 | 41.4 | 447 | 12.9 | 87 | 0.85 | 847 | 2.30 | 1.00 | 684 | 693 | 68.7 |
| | (50) | (3.1) | (67) | (0.9) | (13) | (0.14) | (18) | (1.2) | (0.11) | (45) | (39) | (3.6) |
| | 1013 | 56.7 | 961 | 18.1 | 190 | 1.16 | 1270 | 1.56 | 1.07 | 1288 | 853 | 79.3 |
| | (55) | (8.0) | (196) | (3.0) | (43) | (0.12) | (47) | (1.7) | (0.17) | (113) | (77) | (2.6) |
| | 1251 | 64.9 | 1213 | 20.3 | 237 | 1.28 | 1308 | 1.35 | 1.13 | 1636 | 1103 | 86.7 |
| | (6) | (15) | (406) | (4.5) | (78) | (0.07) | (171) | (0.8) | (0.14) | (210) | (274) | (8.1) |
| RAL | 570 | 9.9 | 122 | 3.2 | 25 | 0.48 | 707 | 29.03 | 0.30 | 407 | 638 | 83.0 |
| | (46) | (2.9) | (31) | (1.1) | (8) | (0.04) | (99) | (7.0) | (0.10) | (87) | (56) | (6.0) |
| | 817 | 30.1 | 376 | 9.1 | 71 | 1.13 | 919 | 3.74 | 1.01 | 752 | 724 | 72.5 |
| | (57) | (5.7) | (77) | (1.7) | (14) | (0.08) | (108) | (3.5) | (0.17) | (123) | (75) | (3.1) |
| | 925 | 36.0 | 509 | 12.0 | 106 | 1.02 | 950 | 3.75 | 0.92 | 882 | 721 | 73.3 |
| | (84) | (8.8) | (264) | (2.6) | (49) | (0.24) | (54) | (2.5) | (0.14) | (125) | (51) | (3.1) |

[a] Values in parenthesis are the Standard Deviation.
[b] MOR = Modulus of rupture (MPa), MOE = Modulus of elasticity (MPa), RS = Breaking resistance (MPa·cm$^3$), EI = Bending stiffness (MPa·cm$^4$), IB = Internal bonding strength (MPa).
[c] HAL = High alignment level ~80%, LAL = Low alignment level ~58%, RAL = Random alignment level ~26%.
[d] DC = Direct-Contact Method, NC = Non-Contact Method, −V = Velocity (m/s), −A = Attenuation (−dB), −R = Root Means Square (volt), −Z = Impedance ($10^{-3}$ Gg/s−m$^2$).

higher velocity than the NC method (Tables 1 and 2) for a given board type. This was probably because of impedance and frequency mismatch caused by pressurized gel-coupling process in the DC method. Such effects are absent in the NC method. The maximum amplitude of the transmitted wave occurs when the "acoustic impedances" of the media are matched. This kind of matching is required for a wave to be transmitted from one medium to another, for example, from liquid to solid (Benson 1991). This result is consistent with observations made by Bhardwaj (1997) and Bhardwaj et al. (2000) that DC ultrasonic velocities are always higher when working with viscoelastic, cellular, and powder-compact materials—particularly when liquids or gels are used as couplants. Under the current setup, the NC system produced a maximum velocity of 1270 m/s, compared with 1670 m/s from the DC system for the same board type. The average impedance (a product of velocity and density) in the DC method had higher values than those from the NC method. For both methods, the impedance was significantly affected by the layering of boards.

Figure 3a shows a general nonlinear relationship between UT velocity and density. The regression curves between UT velocity and density (Fig. 3) showed the distinctive trends segregated by alignment levels for both methods. Particularly, the NC velocity models seemed effective in segregating the random, low, and high alignment levels in the high-density range. Meanwhile, the DC velocity models segregated the alignments well in the mid-density range. This observation suggested that both methods could produce a viable velocity-density model, if flake alignment parameter of the test material is known.

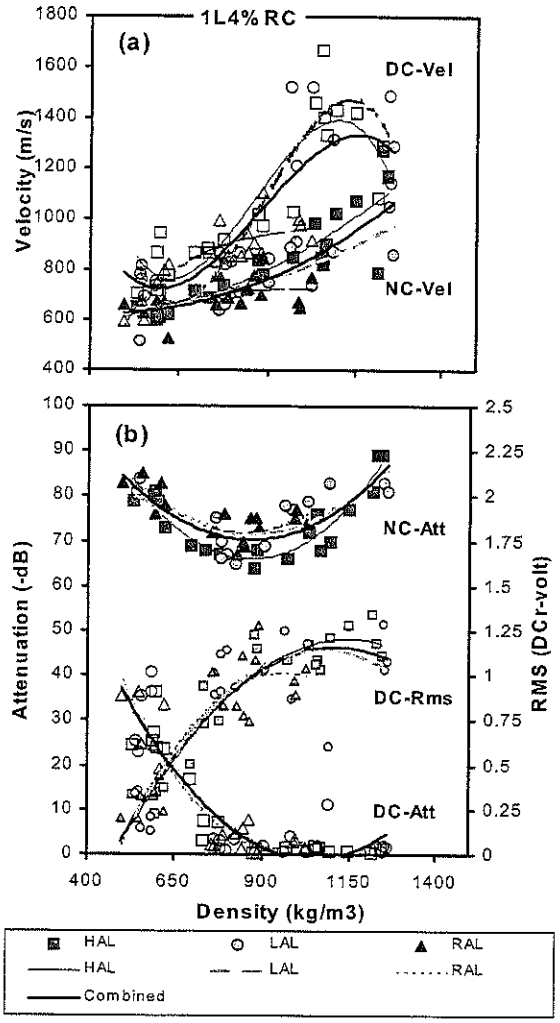


Fig. 3. Scatter plots of the velocity, attenuation, and RMS voltage (r) as a function of average panel density for 4% RC single-layer (1L) panels, segregated by DC and NC methods.

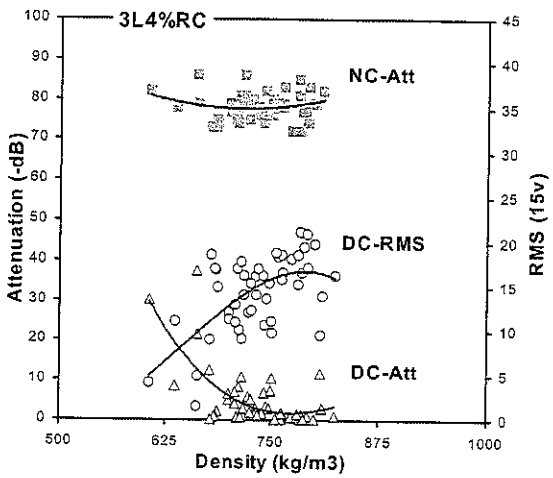


Fig. 4. Scatter plots of the DC and NC attenuation (Att) and DC RMS against density for the three-layer (3L) panels (combined shelling ratios) at the 4% RC level.

### *Attenuation/RMS-density correlation*

Typical non-linear attenuation- and RMS-density relationships in the single-layer panels are shown in Fig. 3b for both methods. The NC attenuation decreased as the density increased, and reached a minimum at about 900 kg/m$^3$. Above the density level, the NC attenuation increased as the density increased further. This indicates certain internal property changes as a result of densification under heating during hot pressing. The DC attenuation decreased and the DC RMS increased as the density increased. Above the 900 kg/m$^3$ density point, both curves leveled off. This further indicates internal property changes above the density level. The density level showed the transition between the diminishing physical effects of the interspatial voids in the lower density half and the increasing plastic-strain hardening modifications in the higher density half. In contrast to the difference in UT velocity, the three-layer panels had similar patterns of attenuation and RMS responses (Fig. 4) as those of single-layer panels.

The DC attenuation-density models had consistently higher $R^2$ values than the NC attenuation-density models (Table 3). The predicted DC attenuation and RMS were invariant to flake alignment changes. This indicated that the DC attenuation and DC RMS were effective in detecting internal properties beyond physical impediments of interfacial boundary of the material. The DC RMS models, approximately inverse to the DC attenuation, showed a better correlation ($R^2 \geq 0.98$) with density for the 1L4%RC panels.

### *Strength-density correlation*

IB strength, bending stiffness (E·I), and breaking resistance (R·S) were highly corre-

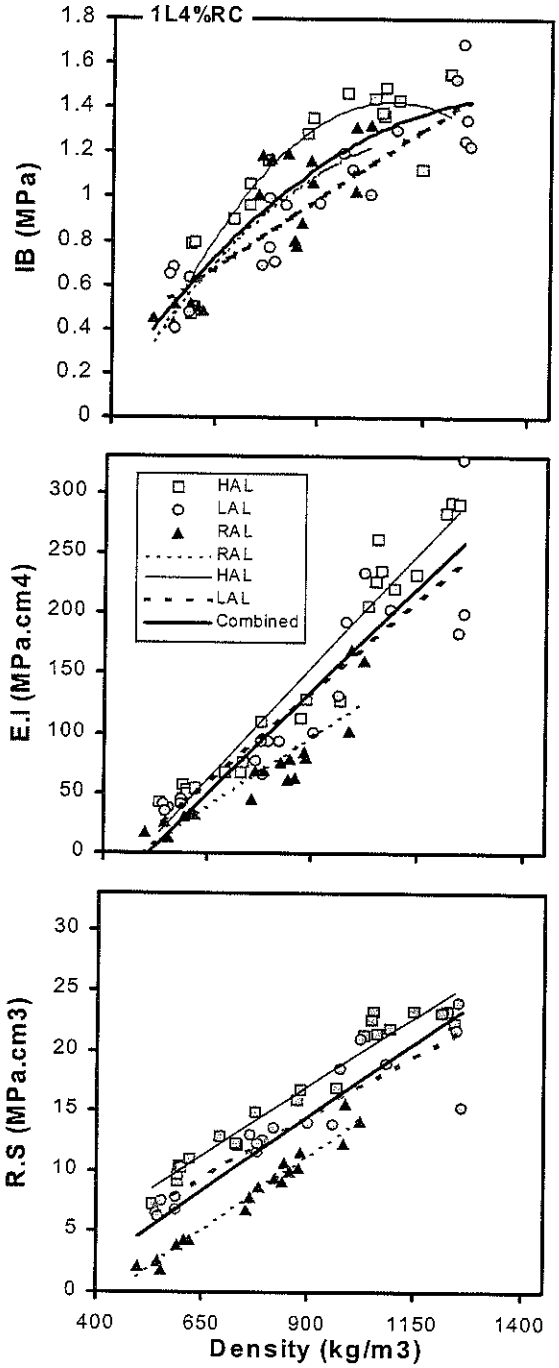


Fig. 5. Scatter plots of internal bond (IB), bending stiffness (E·I), and breaking resistance (R·S) versus density for single-layer boards, segregated by high (HAL), low (LAL), and random (RAL) alignment levels.

Beyond that velocity, the DC curves leveled off significantly indicating that all strength properties became independent of the UT velocity in the density range. The flake alignment levels showed little effects on the relationship. There was also a similar general trend for the NC data.

All three mechanical properties (i.e., IB, EI, and RS) showed an increased trend with DC RMS and a decreasing trend with DC attenuation (Fig. 7). The relationship is generally nonlinear (Table 5). The mechanical properties showed an inconsistent trend with NC attenuation for boards at all flake alignment levels. Flake alignment levels did not significantly influence the UT measurements from both DC and NC methods. Thus, under the current NC settings, strength prediction based on NC attenuation would be inaccurate for OSB products. In the three-layer boards, the NC attenuation showed invariant responses to the panel shelling ratio (i.e., FWR in Table 2). However, the DC attenuation had a minimum value at FWR = 0.5 for the high alignment boards; whereas, the DC RMS had a maximum value.

### *UT parameter-panel property interactions*

Table 6 shows the results of the sensitivity analysis through the backward elimination procedure to show the interactions among the panel properties and UT parameters as influenced by high and low densities in the thickness and horizontal planes of each sample. The average density was strongly correlated to the low and high thickness densities. The low density in both planes significantly affected the bending stiffness of the high-alignment panels. As expected, the high stress concentration was formed in the low density ranges, leading to the bending fracture.

Velocity, in general, was significantly restrained by the low-density points in the thickness direction, especially for the high alignment panels. It was significantly dependent on the high-density area in the horizontal plane for propagation. Particularly, the low-vertical and high-horizontal densities restrained NC

TABLE 5. *Extended.*

| DC – Attenuation (dB) | | | | NC – Attenuation (dB) | | | | DC – RMS (v) | | | |
|---|---|---|---|---|---|---|---|---|---|---|---|
| A | B | C | $R^2$ | A | B | C | $R^2$ | A | B | C | $R^2$ |
| 0.0006 | −0.044 | 1.2006 | 0.81 | −0.0033 | 0.4664 | −15.394 | 0.45 | −0.7664 | 1.8303 | 0.0329 | 0.79 |
| −0.0002 | −0.0077 | 1.0558 | 0.53 | −0.0005 | 0.0888 | −2.7437 | 0.12 | −0.4449 | 1.1318 | 0.3565 | 0.53 |
| 0.0005 | −0.0436 | 1.4392 | 0.84 | 0.0031 | −0.4798 | 19.323 | 0.24 | −0.6341 | 1.8352 | 0.1276 | 0.84 |
| 0.0004 | −0.0342 | 1.2511 | 0.66 | 0.0017 | −0.2628 | 11.105 | 0.06 | −0.3256 | 1.218 | 0.2659 | 0.67 |
| 0.0712 | −4.7309 | 101.12 | 0.49 | −0.572 | 83.914 | −2992.7 | 0.28 | −105.22 | 223.64 | −28.434 | 0.47 |
| 0.0417 | −4.9312 | 162.35 | 0.34 | −0.35 | 55.617 | −2064.2 | 0.16 | −92.287 | 245.65 | −2.2581 | 0.34 |
| 0.2998 | −14.82 | 220.79 | 0.64 | 0.4091 | −58.047 | 2188.7 | 0.18 | 118.97 | 14.777 | 31.077 | 0.68 |
| 0.1659 | −9.6383 | 171.02 | 0.42 | 0.3457 | −49.991 | 1909.7 | 0.07 | 74.356 | 41.141 | 22.96 | 0.45 |
| 0.0054 | −0.4483 | 11.726 | 0.71 | −0.0532 | 7.6543 | −265.28 | 0.46 | −10.586 | 23.827 | −2.5095 | 0.70 |
| 0.0048 | −0.4519 | 17.052 | 0.52 | −0.024 | 3.696 | −126.74 | 0.05 | −5.4168 | 17.237 | 4.0763 | 0.52 |
| 0.0181 | −0.9359 | 21.279 | 0.77 | 0.0217 | −3.206 | 134.26 | 0.06 | 3.6106 | 7.5363 | 6.8702 | 0.79 |
| 0.0103 | −0.6775 | 17.336 | 0.49 | 0.024 | −3.6606 | 151.87 | 0.03 | 3.408 | 7.0564 | 4.6268 | 0.53 |

to characterize OSB's basic properties as influenced by processing variables. All UT responses in relation to the sample density were distributed nonlinearly. DC velocity was higher than the NC velocity, presumably because of transducer or liquid couplant compression effects in the DC method and agglomeration of surfaces as affected by heat and pressure treatments. Generally good models in the single-layer boards were attributed to the nature of the internal structure defined by the uniform density profile and the mean larger density range. The ultrasonic properties were not affected by the panel shelling ratios for the three-layer boards.

The unique DC velocity and NC attenuation responses approaching the inflection density (900 kg/m$^3$) indicated the diminishing effects of the physical voids in the low-density half and the strain hardening in the high-density half. The facts attested that the processing formulation in panel manufacturing, particularly high-density panels, could have definite effects on ultrasonic properties. The strength properties of the boards generally increased with density and flake alignment levels. Viable density models devised in either method were board-specific. Attenuation and RMS were an effective predictor of density if flake alignment level was not known; otherwise the UT velocity could be used.

High density–strength correlations were observed for all board types. The bending stiffness correlated highly to low density points in both thickness and horizontal directions, whereas the breaking resistance correlated well to high sample density. Velocity from both methods depended significantly on the low thickness density, whereas the attenuation/RMS was significantly affected by high and low density boundaries in the thickness direction. The high correlations in both UT–strength and UT–density relationships signal that UT techniques can provide a quick effective assessment of OSB's internal characteristics.

Although the NC system does provide a suitably remote measurement convenience, we recommend that the instrumentation setup and calibration consideration need to match the natural frequency of the test material. With a proper calibration technique, the ultrasonic method is an effective tool for wood composite research and for on-line quality monitoring in fiber-based facilities.

## ACKNOWLEDGMENTS

The financial support to this project by USDA NRI Competitive Grant Program (99-351103-8298) is gratefully acknowledged. The authors wish to thank the SecondWave System Corporation for providing the non-contact ultrasonic transmission measurements,

TABLE 6. *Sensitivity test (in p-values) using backward elimination procedure to evaluate levels of interactions and influences among the structural properties and UT parameters in the high and low densities areas along the thickness and horizontal planes for 4% RC panels.*

| Variables | Alignment level | Vertical-Thickness | | Horizontal-Plane | |
|---|---|---|---|---|---|
| | | Density High | Density Low | Density High | Density Low |
| Stiffness (E.I.) | Combined | 0.0929 | NS | NS | 0.0001 |
| | Random | NS | NS | NS | 0.0001 |
| | Low | NS | NS | NS | 0.0001 |
| | High | NS | 0.0001 | NS | NS |
| Breaking (R.S.) | Combined | NS | NS | NS | 0.0001 |
| | Random | 0.0001 | NS | NS | NS |
| | Low | NS | NS | NS | 0.0001 |
| | High | NS | NS | 0.0001 | NS |
| Ave_Density | Combined | 0.0001 | 0.0001 | NS | 0.0018 |
| | Random | 0.0001 | 0.002 | NS | NS |
| | Low | 0.0036 | 0.0001 | NS | 0.0401 |
| | High | 0.017 | 0.0413 | 0.0012 | 0.0099 |
| DC_Velocity | Combined | NS | 0.0001 | NS | NS |
| | Random | 0.0001 | NS | NS | NS |
| | Low | 0.018 | NS | 0.001 | NS |
| | High | NS | 0.0001 | NS | NS |
| DC_Attenuation | Combined | 0.0022 | 0.0005 | 0.01 | NS |
| | Random | NS | 0.0001 | NS | 0.0156 |
| | Low | 0.0003 | 0.0038 | NS | NS |
| | High | NS | NS | 0.0001 | NS |
| DC_RMS | Combined | 0.0058 | 0.0161 | 0.0722 | NS |
| | Random | NS | 0.0001 | NS | NS |
| | Low | 0.0036 | 0.038 | NS | NS |
| | High | NS | NS | 0.0001 | NS |
| NC_Velocity | Combined | NS | 0.0001 | 0.0132 | NS |
| | Random | NS | 0.0397 | NS | NS |
| | Low | NS | NS | 0.0016 | NS |
| | High | NS | 0.0001 | NS | NS |
| NC_Attenuation | Combined | 0.0012 | 0.0001 | 0.0958 | NS |
| | Random | 0.0006 | NS | NS | 0.0098 |
| | Low | 0.0001 | 0.0001 | NS | NS |
| | High | NS | 0.0088 | 0.0105 | NS |

and Dr. Aravamudhan Raman, Department of Mechanical Engineering, Louisiana State University, for his helpful suggestions.

## REFERENCES

AMERICAN SOCIETY FOR TESTING AND MATERIALS (ASTM). 1996. Annual Book of ASTM Standard D1037-96, American Society for Testing and Materials, Philadelphia, PA.

BEALL, C. F. 1996a. Application of ultrasonic technology to wood and wood-based materials. *In* Ferenc Divos, ed. Proc. 2nd University of Western Hungary International Conference on the Wood Science/Technology and Forestry. Sopron, Hungary.

———. 1996b. Future of nondestructive evaluation of wood and wood-based materials. Keynote pages 409–413 *in* Proc. 10th International Conference on NDE of Civil Structures & Materials, Boulder, CO.

BEAUCHAMP, K. G., AND C. K. YUEN. 1979. Digital methods for signal analysis. George Allen & Unwin Ltd., Boston, MA.

BENSON, H. 1991. University physics. John Wiley & Sons, New York, NY. pp. 663–672; 962 pp.

BHARDWAJ, M. C. 1997. Innovation in non-contact ultrasonic analysis: Applications for hidden objects detection. Mat. Res. Innovation 1:188–196.

———, I. NEESON, AND G. STEAD. 2000. Introduction to contact-free ultrasonic characterization and analysis of consolidated materials. Technical report at the Application of Nondestructive Evaluation in Powder Metals Seminar. Iowa State Univ., Ames, IA. 13 pp.